SLAC–PUB–6721
SLAC/SSRL–0095
October 1994
(SSRL–M)

ANISOTROPIC PHASE SEPARATION THROUGH THE METAL-INSULATOR TRANSITION IN AMORPHOUS ALLOYS

Michael J. Regan*
Marybeth Rice†
Marcela B. Fernandez van Raap‡
Arthur Bienenstock

Stanford Linear Accelerator Center
Stanford Synchrotron Radiation Laboratory
Stanford, CA 94309, U.S.A.

PACS 61.10.Lx, 61.43.Dq, 68.55.-a, 71.30.+h

The characterization of nanometer-scale phase separation in sputtered amorphous metal-Ge and Fe-Si films has led to the observation of a new microstructure that extends through the metal-insulator transition. The phase separated regions, which are dependent on deposition conditions, are well-correlated and of the order of 1 nm in the growth plane but poorly-correlated and 1.5-2.0 nm in the growth direction. The results suggest that fluctuations during film growth play a pivotal role in preventing anticipated columnar structures, probably leading to unusual percolation properties.

Vapor-deposited amorphous metal-germanium and metal-silicon films have been the subject of extensive study over the past decade. Much of the effort is aimed at understanding the metal-insulator (M-I) transition, since many view the films as relatively unique examples of homogeneous materials which undergo a continuous structural transition as the metal concentration is increased. In contrast, Kortright and Bienenstock[1] inferred from their structural study of amorphous Mo_cGe_{1-c} that films with $0<c<0.23$ consist of a-Ge and a Mo-modified material that coexist on a size scale of less than 4 nm. These authors were unable to confirm their supposition definitively with small-angle x-ray scattering (SAXS), however, since the observed intensity patterns could arise from either defects or such phase separation. In addition, they reference an unsuccessful attempt to detect phase separation with transmission electron microscopy. Subsequently, Yoshizumi et al.[2] and Mael et al.[3] noted that their observation of a metallic low temperature specific heat in insulating ($c<0.1$) amorphous Mo_cGe_{1-c} films is consistent with the coexistence proposal.

Recently, Rice et al.[4] have used anomalous small-angle x-ray scattering (ASAXS) to show definitively that a variety of Ge-rich amorphous metal-germanium films have SAXS patterns that arise from composition fluctuations or phase separation, rather than from defects. Electron microscopy has been used in the past to observe composition modulations in, for example, the

Work supported in part by Department of Energy Contract DE-AC03-76SF00515.

Published in *Phys. Rev. Lett.* **73**, 1118 (1994).

amorphous Au-Si system[5], but we focus here on x-ray scattering methods, since anisotropic phase separation, variable electron density contrast, phase compositions and statistical averaging of fine scale modulations are more readily addressed with ASAXS.

We present observations that indicate the M-I transition in the metal-Ge and Fe-Si films probably proceeds by the percolation of an intermetallic phase, as in the granular and partially crystalline Al-Ge materials[6], but on a much finer size scale. Generally, the germanide or silicide intermetallic "particles" are surrounded by a well-defined depletion region (i.e. an insulating phase), so that percolation is by no means simple, as discussed by Deutscher et al.[6] Our measurements also suggest that a theory of phase separation during film growth must take into account fluctuations which interrupt the separation pattern, in addition to those which initiate it. Finally, we demonstrate that one now has the ability to vary the phase separation topology, characterize those variations in spite of the small sizes involved, and study the resulting changes of physical properties.

Amorphous Mo_cGe_{1-c}, Fe_cGe_{1-c}, W_cGe_{1-c}, and Fe_cSi_{1-c} alloys were prepared at room temperature by magnetron co-sputtering of elemental targets onto a rapidly rotating substrate table. Films were grown 1-8 μm thick on Si(100) and Kapton substrates; the metal-Ge films deposited on Si were rendered free-standing by etching the Si substrates in a KOH bath, and, unless otherwise specified, data are from the free-standing samples. The electron microprobe, which samples the top 100 nm of material, and x-ray absorption methods, which sample the entire material, gave compositions within 1-2 at.%, so it does not appear that there is significant drift in metal concentration with film thickness.

The ASAXS data were collected on beamline 4-2 of the Stanford Synchrotron Radiation Laboratory (SSRL). To verify that the SAXS arises from composition fluctuations, ASAXS were acquired with the scattering vector parallel to the film surface plane. For the more complete characterization, a transmission geometry, in which the scattering vector was either normal or oblique to the film surface, was used. These data sets consist of radial scans in $\bar{k}$-space; that is, the sample was taken to a particular tilt angle θ_k so in the small-angle limit the direction of $\bar{k}$ was fixed, and the scattering was measured as a function of $k = 4\pi\sin(2\theta/2)/\lambda$, with 2θ the scattering angle.

For a more complete discussion of sample characterization, ASAXS data acquisition, final data normalization, and large-k power law scattering, see Regan.[7] To isolate the sample's coherent scattering, the method of Maret et al.[8] was used. The large k SAXS for each sample and orientation was fit with a function of the form $A(E,\theta_k)/k^{\alpha} + B(E,\theta_k)$. The B was then removed from each scan, rendering $d\sigma/d\Omega$, the differential cross-section of coherent scatter per sample volume. The data were equally well fit with α values of 4 to 5, and, hence, the coherent scattering was extracted using different values of α to test the sensitivity of physical results to the choice of α.

The composition fluctuation origin of the scattering was confirmed with the ASAXS approach described by Rice et al.[4] For Fe_cGe_{1-c} samples with $c<0.33$, W_cGe_{1-c} with $c<0.20$, and Mo_cGe_{1-c} with $c<0.22$, only slight changes are observed in the magnitude of $d\sigma/d\Omega$ as the incident photon energy is increased beneath the Ge absorption edge while large changes in $d\sigma/d\Omega$ exist for similar changes beneath the metal absorption edges. The insets to figure 1 show the changes in $d\sigma/d\Omega$ at the Ge, Fe, and Mo edges with respect to the changes in the atomic scattering factor, f(E), for three samples at normal incidence. Since there is little, if any, change at the Ge edge, the number density of Ge must be constant throughout the sample. Conversely, the large change at the metal edges is evidence that the SAXS arises from fluctuations in the number density

of metal atoms. The correlations between metal atoms must also be responsible for the marked anisotropy of $d\sigma/d\Omega$ with film orientation, as discussed below. These results imply that, for all samples, voids do not contribute appreciably to the SAXS over this k-range. A more thorough approach using partial structure factors also supports these conclusions.[7]

For the Mo_cGe_{1-c} alloys, we find this scattering in our samples of composition 6.5, 12.4, and 16.5 at.% Mo, while little, if any, scattering is recorded for 23.6 at.% Mo and c>0.24. Similarly, no SAXS was observed for samples with c>0.33 in the Fe_cGe_{1-c} and Fe_cSi_{1-c} samples. This is in contrast to the observations of Lorentz et al.[9] on Fe_cGe_{1-c} for which the Fe had been triode sputtered, as well as our ASAXS observations on the same films, which show large SAXS signals that arise, at least partly, from phase separation. This is one indication of the sensitivity of the phase separation state to the deposition conditions.

Figure 1 shows $d\sigma/d\Omega$ determined from the oblique transmission experiment for several samples near the M-I transition region. The change in the scattering peak with sample orientation indicates that there is strong anisotropy. With the scattering vector "in-plane" (θ_k=90°), there is a strong maximum which shifts inward to smaller k and monotonically decreases in amplitude as the scattering vector is rotated towards the growth direction (θ_k=0°).

We have used three different approaches[7]: cylindrical correlation functions (CCF)[10], dilute inhomogeneous particles and close-packed homogeneous particles, to interpret the anisotropy. Since these give essentially the same physical picture, the focus is on the CCF which is defined as the effective electron density pair correlation function[11], $\gamma(\vec{x},E) = \langle \rho(\vec{x}+\vec{x}_0,E)\rho(\vec{x}_0,E)\rangle$, related to the Fourier transform of $d\sigma/d\Omega$ by the electron scattering length. The effective electron density, $\rho(\vec{x},E)$, accounts for the diminution of the atomic scattering factor that results from anomalous scattering and is determined by the anomalous scattering factors and the relevant number densities in the material. As a result of the vapor deposition process, $\gamma(\vec{x},E)$ is expected to exhibit in-plane isotropy with an axis of cylindrical symmetry in the direction of growth. It is the explicitly cylindrically symmetric $\gamma(\vec{x},E)$, minus its average value, which we refer to as the CCF, and which we have calculated using a spherical harmonics approach.[12] Such functions have been used to study oriented noncrystalline polymers,[13] but to our knowledge have not been applied to vapor-deposited amorphous semiconductors or metals.

In order to focus on the portion of the CCF associated with the phase separation, the CCF has been calculated by extrapolating the observed intensities to infinite k with α=4, after elimination of the background. This CCF contains no information about the atomic structure and assumes that $\rho(\vec{x},E)$ for a particular region is a constant with sharp boundaries between regions of different density.

One immediate result is the mean-square fluctuation of effective electron density, $\gamma(\vec{x}=0,E)$, known as the invariant. If a two phase model is assumed with amorphous Ge or Si as one of the phases, the composition of the other phase can be determined to be close to $FeGe_2$, $FeSi_2$, or $MoGe_3$ in the relevant materials. For a model of sharp interfaces (α=4) and homogeneous distribution of Ge or Si, it is readily shown that

$$\gamma(0,E) = \tfrac{c}{1-c} n_I \left(n_M - \tfrac{c}{1-c} n_I\right) \left|f_M(E)\right|^2,$$

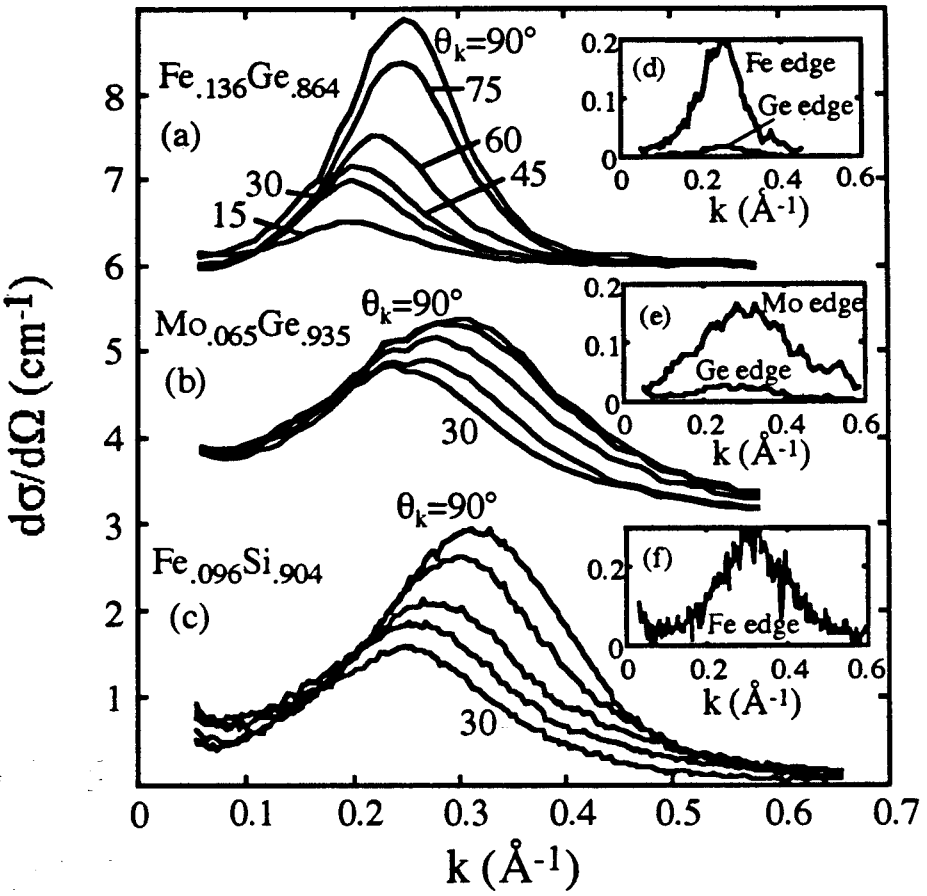

Figure 1. $d\sigma(\vec{k},E)/d\Omega$ (cm^{-1}) as a function of oblique transmission angle for (a) $Fe_{.136}Ge_{.864}$ (E=6912 eV), (b) $Mo_{.065}Ge_{.935}$ (7100 eV), (c) $Fe_{.096}Si_{.904}$ (6912 eV; samples Kapton supported). Data smoothed over an interval Dk=0.02 $Å^{-1}$, offset for clarity, and scaled by an extra 0.25 in (a). (d-f) Absolute changes in SAXS at the Mo, Fe, and Ge K-edges for the samples in (a-c), scaled by the relative change in f(E) at each of the relevant edges.

with I for insulator (Si, Ge) and M for metal (Fe, W, Mo), n_M the number density of metal atoms in the intermetallic, and n_I the number density of I (same in both phases). For a given n_I, n_M can be determined, and hence the composition of the intermetallic phase extracted. For n_I equal to 0.95 and 1.0 times that for c-Si and c-Ge, we calculate endpoints that range from 34 to 38 at.% Fe for the four Fe-Ge alloys we studied, 24 to 27 at.% Mo for two Mo-Ge alloys, and 30 to 35 at.% Fe for four Fe-Si alloys.

We have also calculated $\gamma(\vec{x} = 0,E)$ for α=5, which will help us to place limits on the intermetallic compositions since α is between 4 and 5. With α=5, the transition regions between the minor and major phases would consume ~40-50% of the volume of the minor phase. With a model in which the interfacial region occupies one-half the volume of the intermetallic phase[7] (which is the minor phase for the alloys we studied), we calculate intermetallic endpoints from 32 to 38 at.% Fe for the Fe-Ge alloys and from 23 to 24 at.% Mo for the Mo-Ge alloys.

These two models represent extreme examples of anticipated interfacial regions. They indicate that the compositions of the intermetallic phases are essentially model independent and

appear close to amorphous $FeGe_2$, $FeSi_2$ and $MoGe_3$. This is in agreement with the disappearance of the SAXS for Fe-Si and Fe-Ge compositions greater than 35 at.% Fe and for Mo-Ge alloys with a composition near 24 at.% Mo and are also consistent with the structural model of Kortright and Bienenstock.[1]

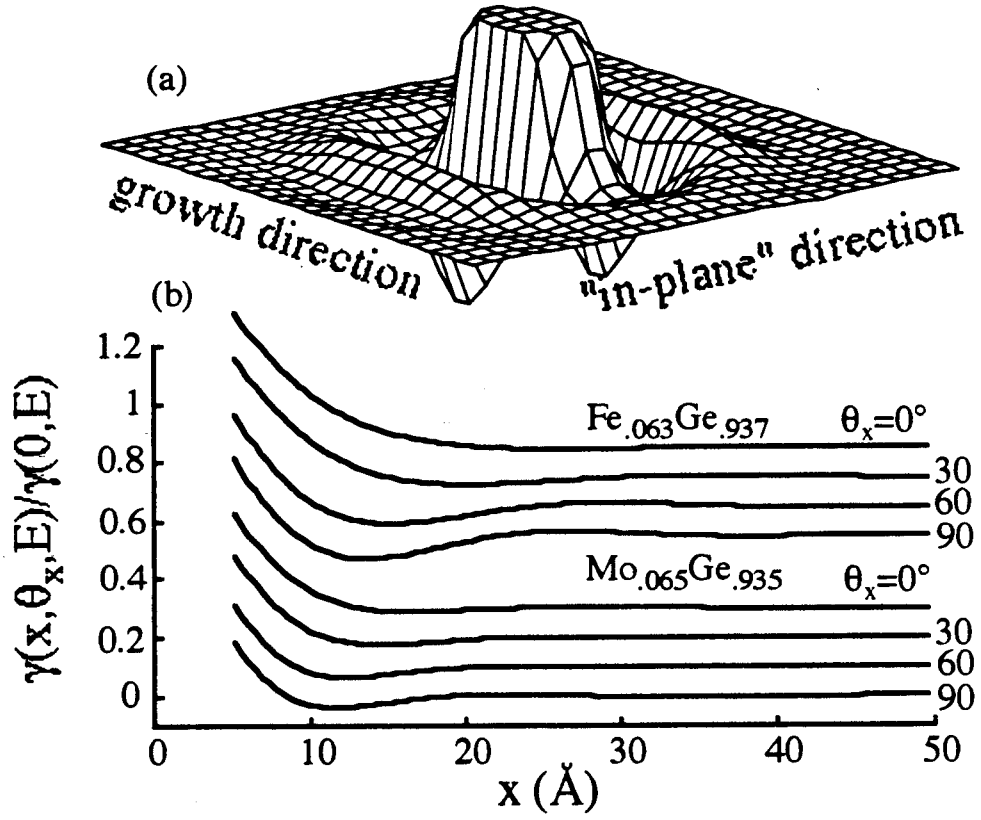

Figure 2. CCF, $g(x,q_x)$, in units of $(e^-/Å^3)^2$. (a) Three-dimensional mesh plot of the CCF for $Fe_{.063}Ge_{.937}$; E=6912 eV. Mesh lines are spaced 4Å by 4Å. (b) $Fe_{.063}Ge_{.937}$ CCF along different radial directions q_x. (c) $Mo_{.065}Ge_{.935}$ CCF along different radial directions; E=7100 eV. Plots offset and truncated at small x in order to better observe the oscillations.

Figure 2 shows the CCF for the $Fe_{.063}Ge_{.937}$ sample as well as sections along the radial direction x as a function of polar angle θ_x (θ_x=90°, $\vec{x}$ in-plane; θ_x=0°, $\vec{x}$ in growth direction) for this sample and one with composition $Mo_{.065}Ge_{.935}$. The large maximum near $\vec{x} = 0$ is from what can be called "intraparticle" correlations. In both alloys, and all others for which we have obtained CCFs, intraparticle correlations extend further in the growth direction than for in-plane directions. If we define the average particle radii as that value of x for which $\gamma(\vec{x} = 0, E)$ has decreased by 90%, then for the $Fe_{.063}Ge_{.937}$ sample, the basic particle radii are 12.7 Å in the growth direction by 7.3 Å in-plane. For the $Mo_{.065}Ge_{.935}$ sample shown in the figure, and a $Fe_{.096}Si_{.904}$ sample, the corresponding dimensions are 8.8 Å by 6.3 Å and 9.9 Å by 5.8 Å, respectively.

Beyond the contribution from self-correlation (x>10Å), oscillations in $\gamma(x,\theta_x)$ about 0 are present. The negative $\gamma(x,\theta_x)$ just outside the intraparticle peak arise from the correlation between a particle and what is usually called a depletion region. The high concentration of metal atoms in the particle, for example, is achieved through diffusion of metal atoms away from the surrounding region, leaving behind a region of lower than average metal density. For all alloys in which CCFs have been obtained, we observe well-defined depletion zones for in-plane correlation vectors, but virtually none for the growth direction. For one of the samples, $Mo_{.065}Ge_{.935}$, we have observed a slightly different behavior, as a small depletion region is evident in the growth direction, in addition to the in-plane direction (fig. 2b). The oscillations beyond this miminum are the subject of work underway.

Given these particle sizes, the overall film compositions, and the recorded absolute intensities, a large packing fraction must exist (also evidenced in our work with particle models[7]). The poorly defined depletion region in the growth direction indicates that little, if any, correlation between particles exists in this direction even though they are rather densely packed. This is likely a result of the deposition process, where the intermetallic particles are formed at the surface by depleting the surrounding area of metal atoms. Then after 2 nm of material have been deposited, fluctuations lead to a new phase separation pattern that is poorly correlated with those buried beneath the surface.

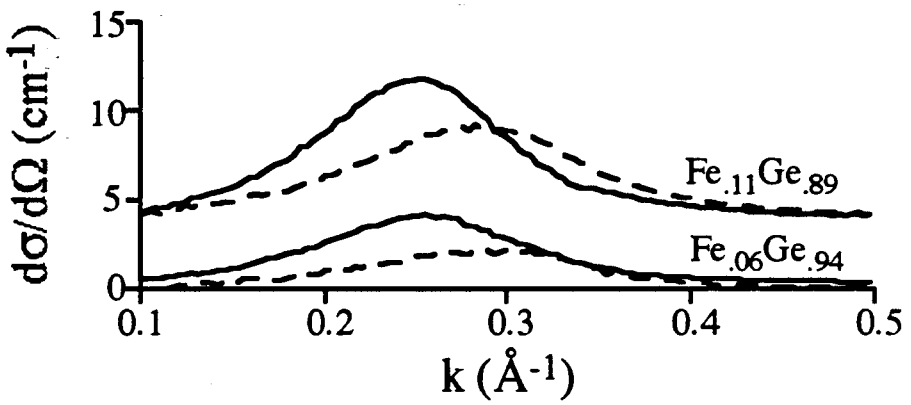

Figure 3. $d\sigma(\vec{k},E)/d\Omega$ (cm^{-1}) as a function of composition and power for several Fe_cGe_{1-c} alloys (E=6912 eV and q_k=90∞, samples Kapton supported, data smoothed over an interval Dk=0.02 $Å^{-1}$). Power delivered to the sputtering targets: æ, 400 watts; – – – 100 watts.

In agreement with this line of reasoning, changes in the deposition conditions can lead to films which are identical in composition but exhibit different states of phase separation. Figure 3 compares the scattering from samples of two compositions that have been prepared with two different Fe and Ge target powers. Samples grown at 400 watts show a more "advanced" state of phase separation than those at 100 watts; that is, the SAXS maximum appears at a smaller magnitude of the scattering vector with greater amplitude.

The formation of in-plane depletion regions is consistent with the surface diffusion picture of in-plane phase separation of Adams et al.[14] This picture, however, leads to a columnar structure, whereas the particles described here are typically only 50% larger in the growth direction than in-plane. This indicates that a more complete theory must incorporate such fluctuations, which might result from, for example, variations in the adatom flux or appreciable sized sputtered metal

clusters.[15] More difficult to understand is the slight depletion region in the growth direction of $Mo_{.065}Ge_{.935}$, which is similar to the "transverse" phase separation observed by Adams et al.[14]

As a consequence of the unusual depletion regions, one would anticipate unique percolation properties. These may account for the differences often cited for the M-I and superconducting transition compositions, for example in amorphous Mo-Ge. Variations in the sizes of the intermetallic and depletion regions with preparation parameters are also a likely cause of the large difference in transition compositions cited by different groups. Finally, it is probably the presence of the intermetallic regions at compositions below the M-I transition composition that accounts for the metallic low temperature specific heat in these materials.

The ability to characterize such fine scale phase separation, as discussed here, leads naturally to the possibility that we may obtain a more thorough understanding of the M-I transition in such systems through systematic variations of deposition conditions, structural characterization and measurements of physical properties.

SSRL is funded by the DOE, Office of Basic Energy Sciences. The Biotechnology Program is supported by the NIH, Biomedical Research Technology Program, Division of Research Resources. Further support is provided by the DOE, Office of Health and Environmental Research. The authors would like to thank P. Lecante and H. Tsuruta. One of us (AB) was a guest of the CNRS Laboratorie de Cristallographie, Grenoble, while this manuscript was being prepared.

*Present address: Division of Applied Sciences, Harvard University, Cambridge, MA 02138
†Present address: Center for X-ray Optics, Lawrence Berkeley Laboratory, Berkeley, CA 94708
‡Present address: Departmento de Fisica, Universidad Nacional de La Plata, c.c. 67, 1900 La Plata, Argentina

[1] J.B. Kortright and A. Bienenstock, Phys. Rev. B **37**, 2979 (1988).
[2] S. Yoshizumi, D. Mael, T.H. Geballe, and R. Greene, in *Localization and Metall-Isulator Transitions,* edited by H. Fritzsche and D. Adler (Plenum, New York, (1985), p. 77.
[3] D. Mael, S. Yoshizumi, and T.H. Geballe, Phys. Rev. B **34**, 467 (1986).
[4] M. Rice, S. Waskatsuki and A. Bienenstock, J. Appl. Cryst. **24**, 598 (1991). M. Rice, Ph.D. Thesis, Stanford University, 1993.
[5] M. Audier, P. Guyot, J.P. Simon, and N. Valignat, J. Phys. Coll. **46**, C8-433 (1985).
[6] G. Deutscher, M. Rappaport and Z. Ovadyahu, Solid State Commun. **28**, 593 (1978).
[7] M.J. Regan, Ph.D. Thesis, Stanford University, 1993.
[8] M. Maret, J.P. Simon, B. Boucher, R. Tourbot, and O. Lyon, J. Phys. Condens. Matter **4**, 9709 (1992).
[9] R.D. Lorentz, A. Bienenstock, and T.I. Morrison, Phys. Rev B **49**, 3172 (1994).
[10] N. Norman, Ph.D. Thesis, University of Oslo, 1954.
[11] A. Guinier and G. Fournet, *Small-Angle Scattering of X-Rays* (Wiley, New York, 1955).
[12] M.J. Regan and A. Bienenstock, J. Phys. IV **3**, 459 (1993).
[13] M.E. Milberg, J. Appl. Phys. **34**, 722 (1962).
[14] See C.D. Adams, M. Atzmon, Y.-T. Cheng and D.J. Srolovitz, Appl. Phys. Lett. **59**, 2535 (1991), and references therein.
[15] See S.R. Coon, W.F. Calaway, M.J. Pellin, and J.M. White, Surf. Sci. **298**, 161 (1993), and references therein.